Mechanics and Mechanical Engineering
Vol. 22, No. 2 (2018) 603–617

https://doi.org/10.2478/mme-2018-0048

Modified Virtual Blade Method for Propeller Modelling

Mateusz Stajuda
Damian Obidowski
Maciej Karczewski
Krzysztof Jóźwik
Institute of Turbomachinery
Lodz University of Technology
Lodz, Poland
mateusz.stajuda@gmail.com

Received (23 June 2018)
Revised (9 July 2018)
Accepted (25 August 2018)

The emergence of large, propeller-based aircraft has revived interest in propeller design and optimization with the use of numerical methods. The flow complexity and computational time necessary to solve complicated flow patterns trailing behind rotating blades, created a need for faster than fully resolved 3D CFD, yet comparably accurate methods for validating multiple design points in shorter time. Improved Virtual Blade Method (VBM) for 2-bladed propeller, including method implementation, analysis and validation against 3D numerical and experimental data is presented. The study introduces adjustments to the original method, accounting for differences between VBM and fully resolved numerical models. These modifications prove to increase the model accuracy for the propeller under consideration and could potentially be applied for different blade configurations as well. The modified Virtual Blade Method allows one to compute the propeller performance with comparable accuracy to 3D CFD computation using only 10% of time needed for one computational point.

Keywords: propeller, CFD, VBM, aerodynamics.

1. Introduction

The Virtual Blade Method (VBM) is a commonly applied design and performance prediction method in propeller and aircraft conception. It is used mostly for helicopters, when assessing the main rotor or propeller performance in different flight regimes as well as for the analysis of main rotor or propeller downwash influence on the aircraft aerodynamics. The method derives from Actuator Disc Model (ADM), which is an analytical approach to modelling rotor performance. The ADM evolved, starting from linear models proposed by Glauert [1] through nonlinear developed by Wu [2] and to even more accurate and advanced models [3, 4]. Development

of semi-analytic models became interesting for researchers with evolution of CFD with Reynolds averaged Navier-Stokes (RANS) equations [5, 6].
The VBM principle is to represent the propeller action on the flow without introducing the actual propeller geometry into the model. Its main advantage is that, coupled with CFD solver, it allows one to perform relatively fast computations for highly complicated flow fields created by rotors to investigate its influence on airframe elements. A reversed case, where aerodynamic influence of airframe elements on rotor performance can also be simulated. The VBM time efficiency comes from lowering the number of mesh elements as a much lower element count can be employed when a physical geometry of a blade is not present in the simulation and does not require mesh refinement near wall boundaries [6]. Well-designed VBM model is capable of cutting down the rotor development time and allows for decreasing the cost of design.
Two different approaches to VBM exist. The pressure disc rotor model approximates a helicopter rotor or propeller in a time averaged manner using inflow and outflow boundary conditions at the disc cylindrical surfaces. This causes a pressure jump across the disc varying with radius and azimuth [5]. Alternatively, a technique that replaces the rotor system with momentum sources modelling the presence of fictitious rotor in all computational cells defining the actuator disc, yielding indirectly a pressure jump across the disc, which varies with radius and azimuth [7, 8]. Both methods determine the rotor forces using the Blade Element Theory [9], using a lookup airfoil table that provides the lift and drag coefficients for the considered blade section.

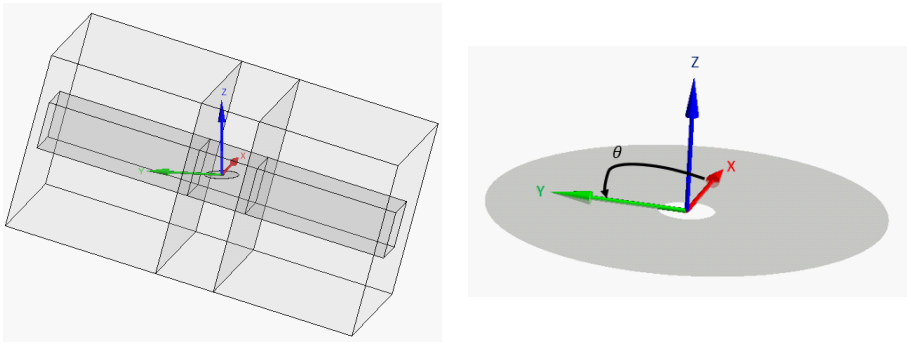

Figure 1 Shapes of: a) external domain geometry, b) disc geometry

2. VBM methodology

The geometry of the simulation domain is shown in Figure 1a and the disc geometry is depicted in Figure 1b. The domain uses opening boundary conditions on all of its walls. The relative pressure for opening is set to 0 Pa. The disc size is equivalent to an area swept by rotor blades, the portion where hub was present is modelled as an impermeable wall. The disc thickness was explicitly set to a

value of 0.01 m to minimize the cross-flow through elements. The disc was meshed using mapped hexahedral mesh to accurately represent the nodes in circumferential direction in order to keep the same radial locations. The disc mesh in vertical direction comprised of one element. The block adjacent to disc was meshed with tetrahedral mesh, while remaining blocks were discretized with hexahedral mesh. The mesh connections between blocks were node to node, without the need for interfaces. The domain walls were modelled as openings, allowing for the fluid to circulate freely, in and out of the domain. The relative pressure on them was set to 0 Pa. The simulations used fully turbulent formulation with SST turbulence model. The simulation setup was developed to allow for forward flight modelling without important changes.

The VBM model was provided with rotor blade specific data as: chord, pitch angle distribution as well as lift and drag coefficients for propeller sections along the blade radius. The values for sections were computed using CFD 2D approach, for only one Reynolds number value for each section, corresponding to expected flow conditions in hover for nominal rotational speed. Re value ranged from $4.5 * e^5$ for the inboard sections up to $1.8 * e^6$ for the propeller tip. The model is, however, capable of incorporating Reynolds number dependent profiles values.

In this implementation, Ansys CFX software was used and source terms were applied to momentum equations in mesh cells corresponding to a propeller disc. The disc was modelled as stationary with respect to the external domain. The momentum sources added to disc mesh cells were computed using Blade Element Method. The velocity values were computed by CFD solver and supplemented with components coming from blade rotation, which was not physically modelled. The added sources were defined in polar coordinate system, shown in Figure 1b. The scheme of computational algorithm is presented in the Figure 2.

The airfoils characteristics is crucial for VBM, as all the results computed by the model rely on them. Therefore high accuracy and reliability is required for profile lift and drag characteristics. The data can be obtained from experimental campaigns or numerical simulations. For the analyzed propeller, limited experimental data were only available for four out of eleven sections. Thus, 2D CFD RANS simulations were used for obtaining the airfoils characteristics. The computational model for profile characteristics used automated numerical procedure for obtaining the solution. The model used RANS solver with fully turbulent formulation and SST turbulence model. Comparison of numerical and experimental data has shown slightly higher lift coefficient prediction by numerical model.

The VBM model relies on velocities computed from CFD flow simulation. For proper reflection of propeller aerodynamics, it was necessary to consider only the velocity component normal to the imaginary blade in every position of the disc, present in plane for each blade section [9]. Therefore different fraction of V_x and V_y had to be accounted for each disc cell. This velocity was composed of two components, V_{xy} acting in the disc plane and the other, V_z normal to the disc plane. The naming scheme is presented in the Figure 3.

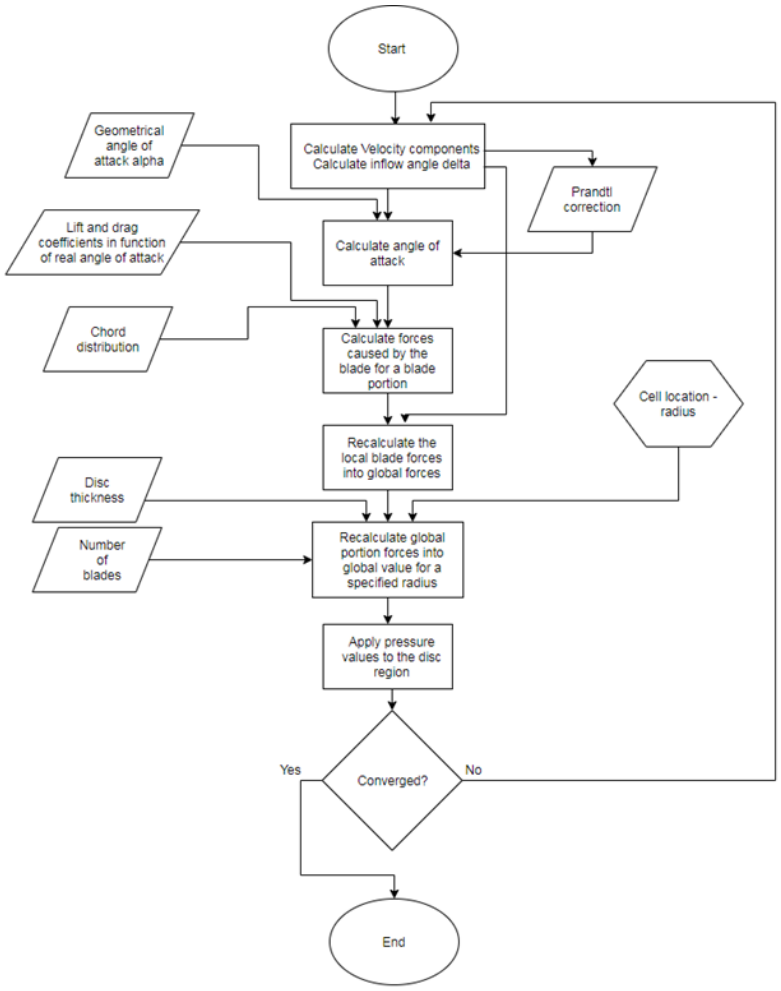

Figure 2 The algorithm of the implemented VBM model

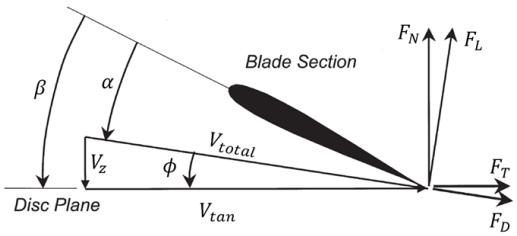

Figure 3 Blade section nomenclature

The velocity V_{xy} was computed according to (1). V_x and V_y for VBM algorithm were taken directly from the cells of the disc. For each cell, local velocity was used. Due to such formulation, the forces on the disc could be recalculated dynamically in case of local velocity changes on the disc surface:

$$V_{xy} = V_x \cos(\theta) \ + V_y \ (-\sin(\theta)) \tag{1}$$

The velocity computed from flow field was supplemented with a velocity resulting from propeller rotation. Therefore the tangential velocity used for computing propeller forces was calculated according to (2):

$$V_{tan} = V_{xy} + \omega R_{local} \tag{2}$$

The inflow angle ϕ was computed using tangential velocity V_{tan} (2) and axial velocity V_z obtained directly from CFD flow solution for a considered cell (3). The angle of attack α was computed by subtracting inflow angle from pitch angle β (4):

$$\phi = \arctan\left(\frac{V_z}{V_{tan}}\right) \tag{3}$$

$$\alpha = \beta - \phi \tag{4}$$

The angle of attack was used for calculating sectional normal and tangential forces exerted by the propeller on the flow. These forces were obtained using equation (5). The lookup table was applied to determine the local chord length $C(R)$ as well as lift and drag coefficients $C_{l(D)}(\alpha, R)$. The chord was a function of radius, whereas lift and drag coefficients were functions of local angle of attack and radius. The force was calculated as per one meter of a blade with specific chord working in specific conditions. Such an approach was required because the force value was further, inside CFX routine, multiplied by the dimensions of a considered cell. The V_{total} value used in (5) is a velocity in the airfoil plane, being a vector sum of V_{tan} and V_z velocities.

$$F_{L(D)} = \frac{1}{2}\varrho\, C(R) V_{total}^2 C_{L(D)}(\alpha, R) \tag{5}$$

Obtained local lift and drag forces were defined in a coordinate system connected with airfoil inflow angle (see Figure 3). They had to be recomputed into disc normal and tangential forces using formulas (6) and (7), incorporating local inflow angle ϕ.

$$F_N = NoB\,(F_L \cos(\phi) \ - F_D \sin(\phi)) \tag{6}$$

$$F_T = NoB\,(F_L \sin(\phi) \ + F_D \cos(\phi)) \tag{7}$$

The forces from (6) and (7) were computed for each mesh cell of the disc. To be applied to the domain, they had to be recomputed into volumetric forces that comply with CFX input requirements. Tangential and normal forces are calculated according to (8) and (9). The denominator results from CFX routine, which multiplies values from (8) and (9) by the cell dimensions, therefore computed forces were divided by disc area and disc height. These equations were used for every cell of the disc, therefore both F_N and F_T have local values, calculated in the cell. The power calculated by VBM (10) has the same form. It uses local tangential force

multiplied by angular velocity and local radius for a cell. Its value is not applied to the flow, but was computed for model validation purpose:

$$F_{N_{volumetric}} = \frac{F_N}{2\pi R\, h_{domain}} \tag{8}$$

$$F_{T_{volumetic}} = \frac{F_T}{2\pi R\, h_{domain}} \tag{9}$$

$$Power_{volumetric} = F_{T_{volumetic}} R_{local}\, \omega \tag{10}$$

Modified version of Prandtl tip correction was used in the VBM model (11) and (12) [9]:

$$F = \left(\frac{2}{\pi}\right) cos^{-1}(e^{-f}) \tag{11}$$

$$f = \frac{NoB}{2}\left(\frac{1-R}{R\phi}\right) \tag{12}$$

The modification comes from substituting the ϕ angle, which is variable in simulation, with a constant value. This is done due to stability reasons, as model formulation with variable ϕ angle would produce cyclic dependency which could result in the lack of convergence of the simulation. Value of F calculated form (11) was multiplied by inflow angle ϕ. This way the inflow angle was reduced near blade tip, as it would happen for a physical blade.

The model was used to obtain results in hover condition. Its outcomes were compared with fully resolved steady state 3D CFD simulations described in previous publication [10] and experimentally obtained thrust and power characteristics. The experiment was a full scale test campaign, where thrust and power values were collected for different propeller operation parameters, including variable rotational speed. Authors had access to partial data, yet this investigation was not done by any of the authors. The VBM computations were performed for three different angular velocities, being 0.84, 1 and 1.16 of nominal propeller rotational speed. The results for computations are presented as thrust and power distributions along the blade, the comparison with experiment is done only using global values.

3. Results

A series of computations was performed for the VBM model. To test its validity, simulations for nominal rotational speed were analyzed. The distributions of velocities and airfoil coefficients are shown in the Figures 4 and 5. It is important that the distributions are close to axisymmetric, with minor disturbances resulting from computed flow velocity differences. The induced velocity flow field at the cross-section perpendicular to rotor disk shown in the Figure 6 proves to be physically valid and is similar to what is expected for a hovering rotor.

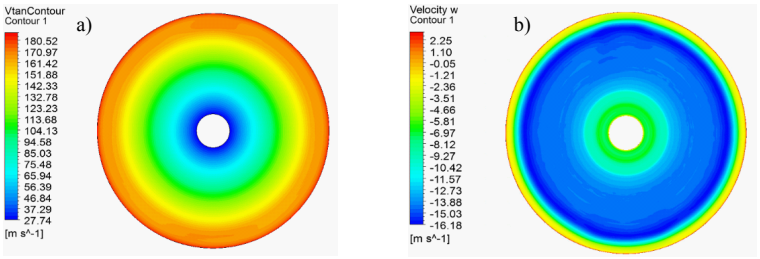

Figure 4 Velocity distribution a) tangential, b) normal

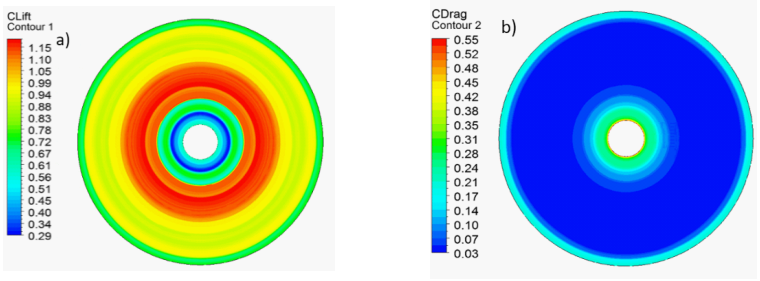

Figure 5 Distribution of a) lift, b) drag coefficients

The flow near to the tip of the propeller (Figure 7) varies slightly from fully resolved 3D CFD simulations [10], mainly due to lack of physical blade geometry in the flow which would change the velocity profile. The tip effect, nevertheless, is partially captured. The comparison is well visible in the Figures 8 to 10, as it shows space-averaged flow data.

The integral of thrust and power was computed in the series of radially bounded volumes. This allowed to plot distribution of these parameters along the blade. Post processed data were used for comparison with fully resolved steady state 3D model [10].

The analysis of results showed expected level of thrust, while power was overestimated by more than 30% (Figures 8 and 9). The reason of difference between power of 3D and VBM model was much higher induced velocity for VBM simulation (Figure 10). Its value had direct influence on ϕ angle, resulting in higher portion of local lift influencing power, according to (7). Due to mutual influence of flow pattern and airfoils characteristics in the model, an attempt to investigate the model sensitivity to airfoil characteristic change was undertaken. After analysis of (6) and (7) it was stated that for the model in discussion, the biggest contribution to power is due to airfoil lift component. The airfoil lift value is also the main contributor to normal force F_N, which reduction may cause a decrease of induced velocity magnitude. The sensitivity study in this aspect used computed profiles lift coefficient, marked

as "1 Cl", 0.9 and 0.8 of these values. These changes were introduced in equation (5), multiplying the lift coefficient by a chosen factor.

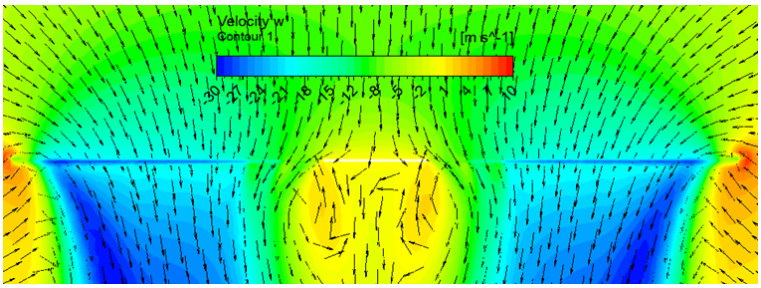

Figure 6 Induced velocity contour with vectors for propeller disc vicinity

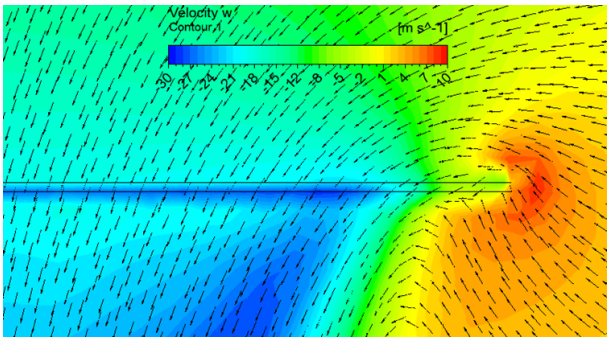

Figure 7 Induced velocity contour and flow field near propeller tip

For each profile value multiplier, the simulation was recomputed to obtain the new flow velocity field along with thrust and power distributions. The results are shown in Figures 8, 9 and 10. It is visible that decreasing the lift coefficient, it is possible to minimize thrust, power and induced velocity component, but velocity still remains overestimated compared to fully resolved model. A C_l value, for which the power is matching the VBM prediction, produces much lower thrust than the value obtained from fully resolved 3D CFD simulation. Since lift coefficient C_l is a main contributor to both thrust and power, a VBM model of such formulation would not be able to reproduce thrust and power values correctly for this particular propeller, regardless of airfoils characteristics. This fact indicates that different approach to modelling is needed.

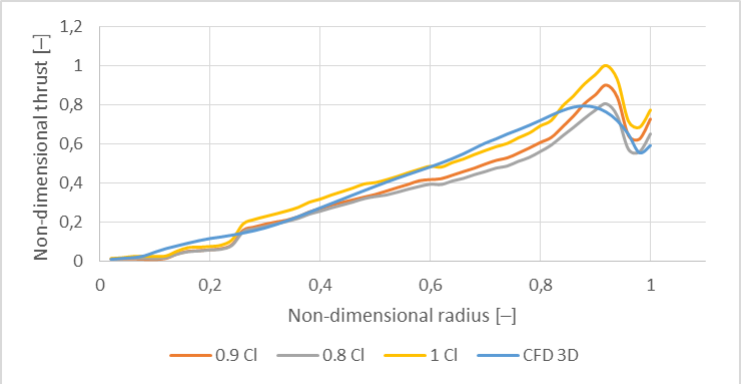

Figure 8 Thrust distribution for variable Cl value

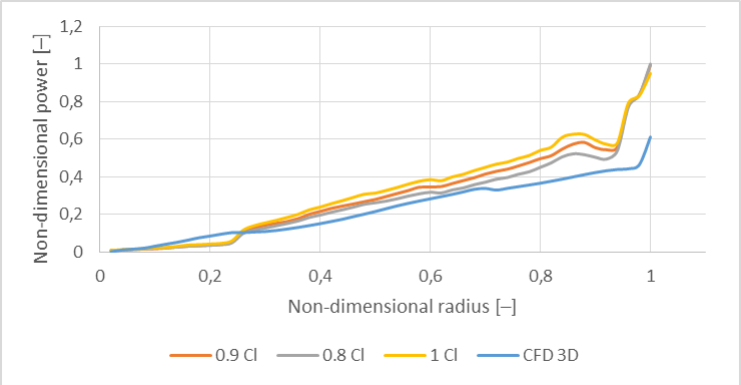

Figure 9 Power distribution for variable Cl value

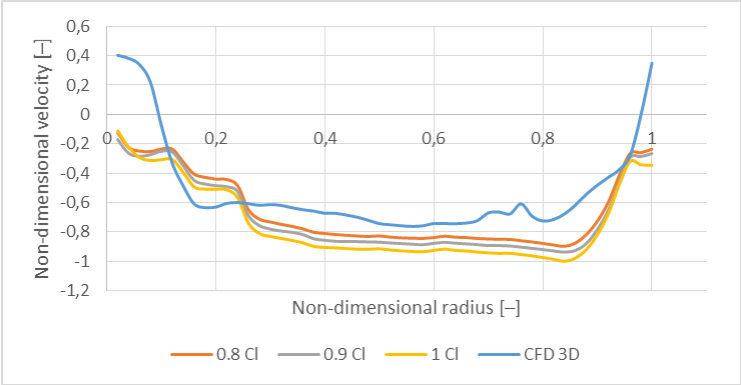

Figure 10 Axial velocity distribution for variable Cl value

4. Modified approach to modelling

From physical point of view, the VBM model would promote higher mass flow through the disc compared to 3D CFD model, as:

1. Blades force is distributed on the whole disc plane, which transfers into lower local force gradients than in fully resolved model, where blades cover only a small portion of the swept area;
2. There is no singularity effect and circulation induced by a blade of finite length (chord-wise);
3. There is no physical blade element in the domain, which could inhibit part of the air flow through the disc.

Therefore a novel attempt to introduce a resistance inside the propeller domain which could compensate for aforementioned mechanisms not reflected in VBM model is proposed. It was assumed that two first mechanisms would be dominant and, therefore, the highest resistance should be present where gradient of pressure is most pronounced. The gradient is strictly connected with computed normal force value, therefore the resistance value should be as well. The value of applied resistance was conceived to be:

$$F_{resistance} = F_{normal} Res \tag{13}$$

where: Res is the resistance parameter, which should be contained within the range from 0 to 1 to maintain proper direction of force action. The values of resistance from 0.1 to 0.4 were tested for the previously described model.
The closest fit of the results was observed for the case with mutual application of resistance and decreasing the values of lift coefficients. The thrust curve for this VBM case with $Res = 0.4$ and $C_l = 0.8$ was below the reference curve for 3D FRM (Figure 11). The power curve for this case was slightly over the reference power curve (Figure 12), yet the difference was significantly smaller than for standard model. To confirm correctness of applied approach, an induced velocity profile was compared for selected VBM model and 3D CFD. The results, shown in the Fig. 13 present very high compliance of velocity profile for $Res = 0.4$ and $C_l = 0.8$ VBM and 3D CFD simulations.

5. Model validation for different rotational speeds

The created model, with $C_l = 0.8$ and $Res = 0.4$, was validated for different rotational speeds to estimate its universality. Due to applied resistance value it was valuable to check whether a value chosen for a given rotational speed would make the model to correctly predict the thrust and power values in different conditions. The values of 0.84, 1 and 1.16 of nominal rotational speed were tested, as the 3D CFD computations for these values were performed [10]. To compare models, thrust, power and induced velocity distributions were plotted. It may be seen (Figure 14) that with increasing rotational speed, the thrust value is underestimated in the region between 50 and 90% of the blade span. Similar aspect is visible in case of power (Figure 15). The situation is different in case of axial velocity (Figure 16), as the difference in this region is not uniform.

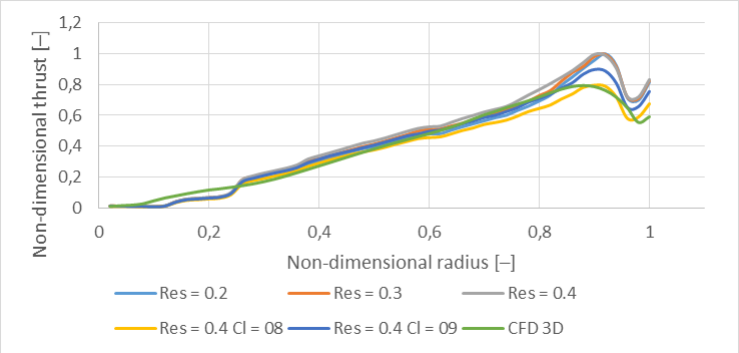

Figure 11 Thrust distribution for variable flow resistance and C_l

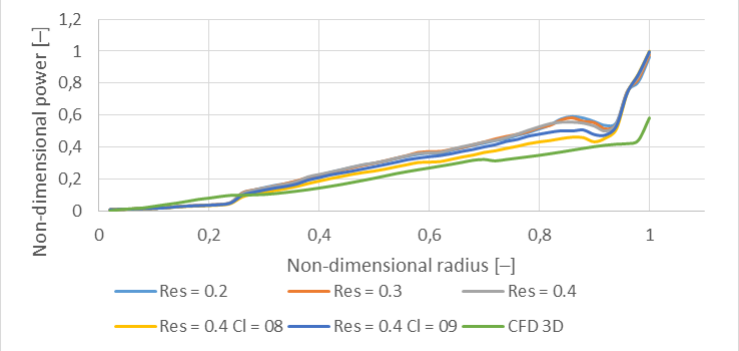

Figure 12 Power distribution for variable flow resistance and C_l

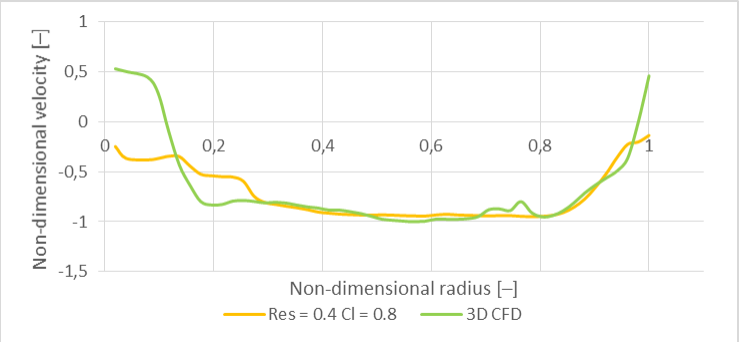

Figure 13 Comparison of induced velocity profiles

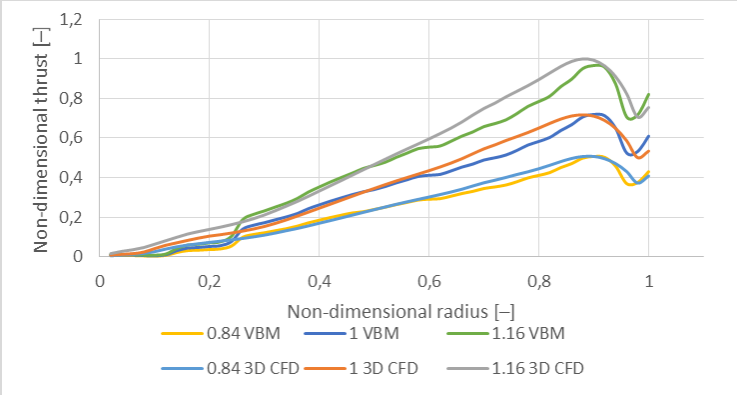

Figure 14 Thrust distribution comparison for different rotational speeds

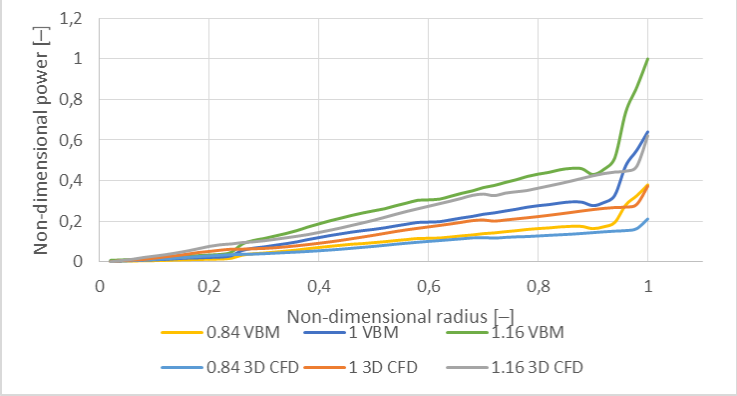

Figure 15 Power distribution comparison for different rotational speeds

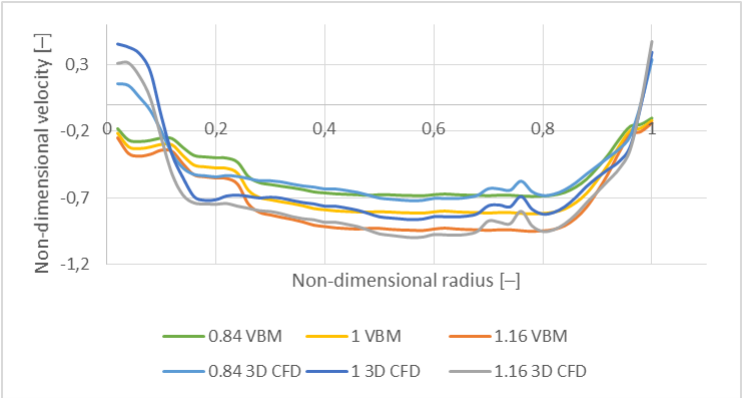

Figure 16 Induced velocity distribution comparison for different rotational speeds

Table 1 summarizes the results from VBM comparing them with results from 3D CFD and experimental data. It may be concluded that the VBM performs best for highest angular velocity, while is severely over predicting power for lowest angular velocity. The model however proves to have non physical characteristics in the region of propeller tip, where very high power is present. This power is attributed to wrongly calculated inflow angle, which results in an increase of power value. Additionally, VBM model results after post-computational removal of power for the last 5% of the blade are included in the Table 1. This shows the model potential if it would not produce such a high error at the propeller tip. The results in this case are much closer to the experimental values.

Table 1 Thrust and power for VBM, 3D CFD expressed in percentage of experimental values

	VBM			CFD 3D	
	Thrust	Power	Power 95%	Thrust	Power
0.84	105%	120%	103%	109%	101%
1	98%	113%	97%	103%	97%
1.16	93%	98%	85%	99%	87%

The modified VBM model provides very similar reliability as 3D simulation, while being able to produce the results significantly faster. Using a workstation class computer with 6 cores at 3.6 GHz the computation time for one operation point was approximately 5 hours, while using 3D CFD approach it increased to over 48 hours.

6. Conclusions

A standard VBM modelling technique described in literature [5, 6] and implemented in Ansys CFX proved to produce results highly inconsistent with numerical reference as well as experimental values for 2-bladed propeller analysis. The problem is mainly overestimated induced velocity value, which resulted in poor blade performance prediction as compared to experiment or 3D CFD. Due to this fact, a modified approach to VBM modelling was proposed.

New modelling approach relies on introducing additional resistance coefficient to the flow to the blade thrust force. Using this approach it was possible to obtain much better results than without the resistance. For nominal angular velocity, the difference between numerical and experimental value was 2% under prediction for thrust and 12% over prediction for power. The power characteristics proved to be nonphysical in the region of propeller tip, producing very high power values at the last 5% of blade radius. Disregarding the values coming from this region, the difference for power was 3% lower than in experiment. It is therefore stated that overall propeller performance in other blade parts was predicted correctly and further model improvement may be required in the region of propeller tip.

The created model, tuned for nominal rotational speed, proved to work reasonably well also for different speeds in hover condition, producing reliable results of

comparable quality as fully resolved 3D CFD model. Once again, the performance at propeller tip was nonphysical, but comparison of data disregarding the power generated at the last 5% of the blade proved to give good approximation, under predicting the power for higher rotational speeds. This may result from the fact, that the power generated at the tip should not be totally neglected. This topic is however very subtle and requires further analysis as the model would be perfected. Both simulation methods – 3D CFD and VBM model produce predictions which discrepancy from experimental results vary with rotational speed. It may be caused by additional physical phenomena, happening in real test conditions and not included in the numerical simulation. Those may be for example geometrical changes of the blade shape, which would be more pronounced for increasing rotational speed, and therefore centrifugal force and aerodynamic blade loading. The other reason of the discrepancy can be lack of rotor head in CFD and VBM that was present in experiments.

Created model should be tested for different propellers and flight conditions to ensure its reliability for a broader range of cases. It is possible that resistance value will be a function of propeller geometry and number of blades. For performing such a delicate analysis, it could be needed to obtain additional data from transient CFD simulations, as the predictions of propeller performance should be independent of geometrical parameters of the domain. It has been shown that the steady state 3D CFD simulations are not meeting this condition [10]. The potential of this method is very high, especially when multiple design points are to be computed. It is significant that proposed modelling approach with altered propeller disc formulation allows one to obtain much better results for this particular case than the approach described in literature.

References

[1] **Glauert H.**: Airplane propellers, in W. F. Durand (Ed.), *Aerodynamic theory, Berlin: Springer*, IV, Division L, 169–360, **1935.**

[2] **Wu T. Y.:** Flow through a heavily loaded actuator disc. Schiffstechnik, 9, 134–138, **1962**.

[3] **Conway J. T.:** Exact actuator disk solutions for nonuniform heavy loading and slipstream contraction, *J FLUID MECH*, 365, 235–267, **1998**.

[4] **Breslin J. P., & Andersen P.**: Hydrodynamics of ship propellers, *Cambridge University Press*, **1994**.

[5] **Le Chuiton, F.**: Actuator disc modelling for helicopter rotors, *AEROSP SCI TECHNOL*, 8, 4, 285–297, **2004**.

[6] **Wahono, S.**: Development of Virtual Blade Model for Modelling Helicopter Rotor Downwash in OpenFOAM, No. DSTO-TR-2931, *DEFENCE SCIENCE AND TECHNOLOGY ORGANISATION FISHERMANS BEND (AUSTRALIA) AEROSPACE DIV*, **2013**.

[7] **Zori, L. A. J., Rajagopalan, R. G.**: Navier-Stokes Calculation of Rotor-Airframe Interaction in Forward Flight, *J AM HELICOPTER SOC*, 40, **1995**.

[8] **Yang, Z. et. al.**: Recent improvements to a hybrid method for rotors in forward flight, *J AIRCRAFT*, 39, 5, 804–812, **2002**.

[9] **Leishman, G. J.**: Principles of helicopter aerodynamics with CD extra, *Cambridge University Press*, **2006**.

[10] **Stajuda, M. et al.**: Development of a CFD model for propeller simulation, *Mechanics and Mechanical Engineering*, 20, 4, 579–593, **2016**.

Nomenclature:

α – angle of attack
β – pitch angle
ϕ – inflow angle
ω – rotational speed
θ – angular position in disc plane
ϱ – density
c – chord of an airfoil
C_L – lift coefficient
C_D – drag coefficient
f – Prandtl correction exponent
F – Prandtl correction factor
F_D – drag force
F_L – lift force
F_N – thrust force
F_T – force tangential to the disc plane
F_{Res} – resistance force applied to the fluid in disc domain
h_{domain}- disc domain height
NoB – number of blades
R (R_{local}) – propeller radius (local propeller radius)
Res – resistance value
V_{xy} – flow velocity in the disc plane
V_{tan} – velocity in the disc plane, including rotational component
V_x – velocity in global X direction
V_y – velocity in global Y direction
V_z– axial velocity, perpendicular to the disc plane
V_{total} – total velocity for profile section
CFD – computational fluid dynamics